
CHAPTER 9

Population Dynamics of
Tribolium

Robert A. Desharnais

The study of population dynamics is complicated by the difficulty of obtaining experimental evidence that supports the predictions of mathematical models. Biologists are faced with numerous challenges such as sampling error, environmental fluctuations, and lack of replication in the study of populations in the field. One approach to this problem is to examine experimental populations under controlled laboratory conditions. Flour beetles of the genus *Tribolium* are an excellent experimental system for evaluating predictions of demographic models.

The flour beetle has a long history in population biology. Royal Norton Chapman (1928) introduced *Tribolium* as an experimental insect for the study of population growth. Age structure in flour beetles was first investigated by John Stanley (1932), a student of Chapman. Thomas Park (1948) began an extensive series of experimental investigations on species competition involving *T. castaneum* and *T. confusum*. Reviews of the vast literature that has developed on *Tribolium* can be found in the papers by King and Dawson (1972), Mertz (1972), and Bell (1982) and in the books by Sokoloff (1972, 1974, 1977) and Costantino and Desharnais (1991).

There are several reasons for the popularity of *Tribolium* as an animal model for the study of populations. Cultures can be maintained indefinitely on a simple medium of flour and yeast. The insects undergo a holometabolous development from egg to adult in four to six weeks. Adults are about 3 mm in length; hundreds of insects can be maintained on 8–20 grams of flour. An accurate census of the population is obtained by sifting the medium and counting the life stages. Large numbers of replicate cultures can be kept

in an unlighted incubator under constant conditions of temperature and humidity. Several species, mutants, and genetic strains are available. Much is already known about the basic anatomy, taxonomy, physiology, development, genetics, and ecology of this beetle (Sokoloff 1972, 1974, 1977).

This chapter focuses on one specific area of population research involving *Tribolium*: nonlinear demographic dynamics. The emphasis is on approaches and results appropriate to the theme of "structured-population models" found throughout this book. A comprehensive review of the literature is not attempted; this chapter deals mostly with the work of my colleagues and me (for more in-depth treatment of these subjects, see Costantino and Desharnais 1991).

The chapter is divided into four parts. It begins with a brief description of the life-stage interactions that occur in flour beetle cultures. The remaining three sections illustrate different approaches that have been used to model these interactions. The first (used in Desharnais & Liu 1987) is based on the classic Leslie matrix model for age-structured populations. The next section describes the integral-equation model of Hastings (1987) and Hastings and Costantino (1987) for the cannibalism of eggs by larvae; this is referred to as the "egg-larval submodel." The last section deals with the more recent results of Costantino et al. (1995), Cushing et al. (in press), and Dennis et al. (1995), which are based on the "LPA model," a system of three difference equations for the dynamics of the larval, pupal, and adult life stages. Each of these approaches represents a different trade-off between biological complexity and mathematical tractability.

1 Life-Stage Interactions

One of the most compelling reasons for using *Tribolium* in the study of populations is that it provides a fascinating example of nonlinear demographic dynamics. Laboratory populations maintained under constant environmental conditions usually exhibit dramatic fluctuations in density and age structure. These fluctuations cannot be characterized as stochastic; they are the result of strong behavioral and physiological interactions among the life stages—the most important being cannibalism.

The life-stage interactions that drive the dynamics of *Tribolium* populations are summarized in Figure 1. The open arrows represent the life cycle, which, for *T. castaneum* at 34°C, has a duration

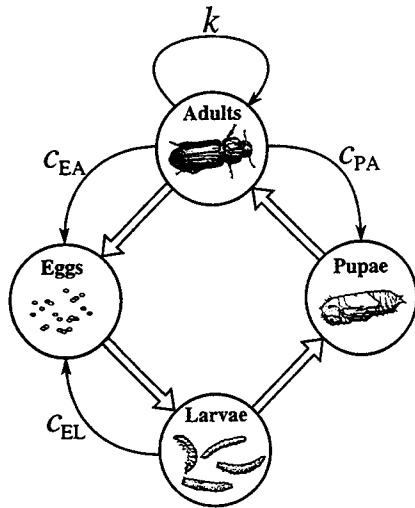


FIGURE 1. Life-stage interactions in *Tribolium*.

of approximately 28 days. The single arrows represent the interactions. The arrows labeled c_{EA} and c_{PA} represent the cannibalism of eggs and pupae, respectively, by adults. The arrow labeled c_{EL} represents the cannibalism of eggs by larvae. Pupal cannibalism by larvae occurs at a much lower rate; for simplicity, it can be ignored. The fecundity of females decreases with crowding; this is represented by the arrow labeled k .

An important consequence of these life-stage interactions is that *Tribolium* populations rarely reach the "carrying capacity" of their laboratory "habitat." As the number of adult beetles increases, the effects of cannibalism and reduced fecundity cause decreases in adult recruitment. As an example, consider adults eating pupae, ignoring for the moment the other life-stage interactions. If b denotes the number of pupae produced per adult, then the number of potential adult recruits is bN , where N is the adult number. However, these pupae must survive cannibalism by adults. Ignoring subscripts, let c denote the probability that a given adult will find and eat a given pupa in some fixed time interval. The probability that the pupa is not eaten by the adult is $1 - c$. If N adults are present during the time interval, then the probability that the pupa avoids being eaten by any of the adults is $(1 - c)^N$, which, if c is small, is approximately equal to e^{-cN} . The total number of re-

cruits into the adult population becomes bNe^{-cN} , which decreases toward zero as $N \rightarrow \infty$. The same argument holds for the other life-stage interactions. A common observation is that the most cannibalistic species and genetic strains of *Tribolium* are the ones with the lowest population densities (Park et al. 1965; Costantino & Desharnais 1991). This negative exponential function appears throughout the *Tribolium* literature.

2 Leslie Matrix Model

An earlier model (Desharnais & Liu 1987) of the demographic dynamics of *Tribolium* populations was based on the projection-matrix approach introduced into biology by Bernardelli (1941), Lewis (1942), and Leslie (1945). In this model, the beetle life span is divided into ω age classes, where each age class spans a single day. The population is represented by a $\omega \times 1$ vector $\mathbf{n}(t)$, whose elements are the densities of each age class at time t . A Leslie matrix $\mathbf{M}(t)$ is used to project the age structure forward one unit of time (one day). The dynamics are given by the matrix equation

$$\mathbf{n}(t+1) = \mathbf{M}(t)\mathbf{n}(t), \quad (1)$$

which, in expanded form, is

$$\begin{pmatrix} n_1(t+1) \\ n_2(t+1) \\ n_3(t+1) \\ \vdots \\ n_\omega(t+1) \end{pmatrix} = \begin{pmatrix} b_1(t) & b_2(t) & \cdots & b_{\omega-1}(t) & b_\omega(t) \\ s_1(t) & 0 & \cdots & 0 & 0 \\ 0 & s_2(t) & \cdots & 0 & 0 \\ \vdots & \vdots & \ddots & \vdots & \vdots \\ 0 & 0 & \cdots & s_{\omega-1}(t) & 0 \end{pmatrix} \begin{pmatrix} n_1(t) \\ n_2(t) \\ n_3(t) \\ \vdots \\ n_\omega(t) \end{pmatrix}. \quad (2)$$

The $b_i(t)$'s and $s_i(t)$'s are age-specific values for fecundities and survival probabilities, respectively, which, in general, vary in time.

The strategy of the 1987 model was to represent the vital rates of the Leslie matrix by functions that capture the basic biology described in Figure 1 using as few parameters as possible. Parameters were estimated from data, and the model simulations were compared with experimental results. Inferences about the effects of life-stage interactions on the demographic dynamics of populations were obtained using numerical simulations to explore the model's behavior in various regions of parameter space. (A more general description of this model can be found in Costantino & Desharnais 1991.)

The first step is to group the age classes into life stages. Based on estimates of the life-stage durations for the corn oil sensitive (*cos*) mutant of *T. castaneum* (Moffa 1976), the life stages can be approximated using the following sets of integers: $E = \{1, 2, 3\}$ for eggs, $L = \{4, 5, \dots, 23\}$ for larvae, $P = \{24, 25, 26\}$ for pupae, and $A = \{27, 28, \dots, \omega = 300\}$ for adults. The densities of each stage are obtained by summing the age vector over these sets:

$$N_J(t) = \sum_{i \in J} n_i(t), \quad J \in \{E, L, P, A\}.$$

For example, $N_L(t)$ and $N_A(t)$ are the number of larvae and adults, respectively.

Fecundity rates depend on the age of females and are reduced by the effects of crowding. The data of Moffa (1976) suggest that, for the *cos* strain, the fecundity of female adults decreases linearly with age. Rich (1956) showed that the fecundity rates of *T. confusum* females decrease as the density of adults increases. These results lead to the parameterization of the fecundity terms (Desharnais & Liu 1987) using

$$b_i(t) = \begin{cases} [\alpha - \beta(i - \varepsilon)] \exp[-kN_A(t)] & \text{for } i \in A, \\ & i \leq \varepsilon + \text{int}(\alpha/\beta), \\ 0 & \text{otherwise,} \end{cases} \quad (3)$$

where α is the maximum fecundity rate per adult (one-half the number of eggs laid per female per day), β is the slope of the linear decrease in fecundity with age, k is a parameter describing the sensitivity of fecundity to the effects of crowding, $\varepsilon = \min(A)$ is the age at which a beetle enters the adult stage, and "int" is the integer function. These fecundity values comprise the first row of the Leslie matrix in equation (2).

Survival probabilities involve both "natural" (nonpredatory) mortality and death due to cannibalism. In the absence of cannibalism, the survival probabilities of eggs and pupae are usually high (Moffa 1976); for simplicity, no natural mortality is assumed for these two life stages. Larvae and adults are assigned natural mortality rates of μ_L and μ_A , respectively. The rate at which a larva consumes eggs depends on the age of the larva; older, larger larvae are more voracious cannibals of eggs. Let $c_{EL}(j)$ denote the cannibalistic rate of a larva of age j . Using the data of Park et al. (1965) for four genetic strains of *T. castaneum*, $c_{EL}(j)$ can be approximated as a linearly increasing function of age: $c_{EL}(j) = c_{EL}'(1 + j - \zeta)$,

where c'_{EL} is the slope of the linear increase and $\zeta = \min(L)$, the age at which a beetle enters the larval stage (Desharnais & Liu 1987). It is assumed that the rates c_{EA} and c_{PA} , at which an adult cannibalizes eggs and pupae, respectively, are independent of the age of the adult. With these assumptions, the survival probabilities are

$$s_i(t) = \begin{cases} \exp\left[-c'_{EL} \sum_{j \in L} (1+j-\zeta)n_j(t) - c_{EA}N_A(t)\right] & \text{for } i \in E, \\ \exp(-\mu_L) & \text{for } i \in L, \\ \exp\left[-c_{PA}N_A(t)\right] & \text{for } i \in P, \\ \exp(-\mu_A) & \text{for } i \in A, \\ & i \neq \omega. \end{cases} \quad (4)$$

These probabilities form the subdiagonal of the Leslie matrix in equation (2).

Data from several sources are used to estimate the parameters in (3) and (4) (Desharnais & Liu 1987). Table 1 lists these parameters, their estimates and standard errors, and a reference to the source of the data. Whenever possible, data on the *cos* strain of *T. castaneum* were used. However, the estimate of the rate of egg cannibalism by larvae was obtained from the data of Park et al. (1965) for four different genetic strains of *T. castaneum*, and the estimates of the parameters for crowding and egg cannibalism by adults were obtained from the data of Rich (1956) for the species *T. confusum*. (For details on how the numerical estimates and standard errors were computed, see Desharnais & Liu 1987; Costantino & Desharnais 1991.)

It is possible to make inferences about the rate of population growth under "density-independent" conditions. If one sets the parameters k , c_{EL} , c_{EA} , and c_{PA} equal to zero, the vital rates in the Leslie matrix \mathbf{M} become constants, and one obtains the classic linear model of geometric growth. The net reproductive rate is given by $R_0 = \sum_{i=1}^{\omega} s_{i-1}b_i$, where $s_0 = 1$. Assuming a 1:1 sex ratio, this equals half the number of eggs a female beetle is expected to produce in her lifetime. The daily rate of population increase, λ_0 , is the dominant eigenvalue of the matrix \mathbf{M} , and the intrinsic rate of increase per day, r_0 , is the natural logarithm of this eigenvalue. For the estimates in Table 1, we obtain $R_0 = 185.5$, $\lambda_0 = 1.140$, and $r_0 = 0.131$ per day. A female is expected to produce approx-

TABLE 1. *Parameter Estimates for the Leslie Matrix Model*

Parameter	Description	Estimate (\pm SE)	Source of Data
μ_L	larval mortality	0.0251 ± 0.0020	Desharnais & Liu (1987)
μ_A	adult mortality	0.0130 ± 0.0009	Desharnais & Costantino (1980)
α	maximum fecundity	7.96 ± 0.20	Moffa (1976, p. 51)
β	decrease in fecundity with age	0.0664 ± 0.0028	Moffa (1976, p. 51)
k	decrease in fecundity from crowding	0.00164 ± 0.00006	Rich (1956, Table IV)
c'_{EL}	larval cannibalism of eggs (slope)	0.000760 ± 0.000047	Park et al. (1965, Table 10)
c_{EA}	adult cannibalism of eggs	0.00252 ± 0.00016	Rich (1956, Table IV)
c_{PA}	adult cannibalism of pupae	0.00558 ± 0.00026	Jillson & Costantino (1980)

imately 371 eggs in her lifetime. Once a constant age distribution is obtained, the population density increases by 14 percent each day—a prolific rate of growth. It is clear why flour beetles are such an important pest of stored grain and food products. These conclusions are consistent with other estimates for *T. castaneum* cultured at the same temperature and humidity (Sokoloff 1974, Table 11.22).

Predictions were obtained for the equilibrium densities and population stability. A unique equilibrium age vector $\mathbf{n}^* > \mathbf{0}$ exists if and only if $R_0 > 1$ (Desharnais & Liu 1987). Determining the stability of this equilibrium requires calculating a “stability matrix” \mathbf{S} whose elements are the coefficients of a “linearization” of the model

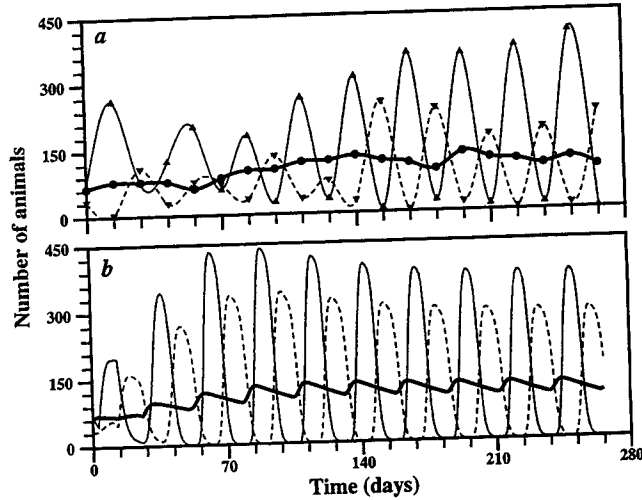


FIGURE 2. Densities of adults (heavy lines), large larvae plus pupae (dashed lines), and small larvae (thin lines) for (a) control replicate "A" (Desharnais & Liu 1987) and (b) the Leslie matrix model. (a) circles, triangles, Census points; curves, interpolating cubic splines.

in the neighborhood of \mathbf{n}^* . The eigenvalues of \mathbf{S} determine the stability of the equilibrium; if the modulus of the dominant eigenvalue is less than one, the equilibrium is stable. Estimates of the parameters have been used to provide expressions for computing the elements of \mathbf{n}^* and \mathbf{S} (Desharnais & Liu 1987; Costantino & Desharnais 1991). When grouped into life stages, the predicted equilibrium densities are 430 eggs, 134 larvae, 10 pupae, and 88 adults, which are within the ranges normally observed for this species. However, this equilibrium is unstable; the dominant eigenvalues are the complex conjugates $\lambda_1, \lambda_2 = 1.00 \pm 0.23i$ with a modulus of 1.03. The largest subdominant eigenvalues are $\lambda_3, \lambda_4 = 0.99 \pm 0.02i$ with a modulus of 0.99. All the remaining eigenvalues are complex and unique. The linearized stability analysis predicts an unstable equilibrium.

The model's demographic dynamics show good qualitative agreement with those observed in the laboratory. Figure 2 is a plot of the life-stage densities for control replicate "A" of an earlier experiment (Desharnais & Costantino 1980) and the Leslie matrix model. For this comparison, the larval age class is divided into two

TABLE 2. *Bifurcation Values for the Leslie Matrix Model*

Model Parameter	Bifurcation Value	Ratio to Estimated Value	Effect of Increasing the Parameter
μ_L	0.0788	3.14	stabilize
α	0.718	0.0902	destabilize
k	0.0211	12.9	stabilize
c_{EL}	0.000146	0.192	destabilize
c_{EA}	0.00896	3.56	stabilize
c_{PA}	0.187	33.5	stabilize

groups of equal duration. The number of pupae is combined with the number of large larvae. Cubic splines interpolate the census data, which were collected every two weeks. Large oscillations in the number of immatures are evident. Smaller oscillations in the number of adults are predicted by the model; these low-amplitude oscillations are not obvious in the census data. With respect to the magnitudes of the life-stage oscillations, there is good agreement between the model and the census data. The same observation can be made for additional data on four control populations and nine populations subjected to demographic perturbations (Desharnais & Liu 1987). Overall, the model does a good job of capturing the qualitative behavior of the life-stage densities.

Numerical analyses of the Leslie matrix model provide information on the effects of each parameter on demographic stability. Varying each parameter singly, while keeping the remaining parameters at their estimated values, and employing a simple bisection searching algorithm, "bifurcation points" can be located at which the equilibrium loses stability (Desharnais & Liu 1987). The results are presented in Table 2. Oscillations persist for all values of β and μ_A , so these parameters are absent from the table. Increasing the rate of reproduction, α , or the rate at which larvae eat eggs, c_{EL} , has a destabilizing effect; increasing the remaining parameters stabilizes the model. The ratios of the bifurcation values to the estimated values suggest that large modifications of the parameters would be required to stabilize the model; the laboratory populations lie well within the unstable region of parameter space.

A significant drawback of the nonlinear Leslie matrix model is that it is analytically intractable. A local stability analysis requires the calculation of the eigenvalues of a 300×300 matrix. Laborious numerical simulations are required to gain some modest information on the effects of the parameters on population growth; a systematic mapping of parameter space is not practical. So although the model includes several biologically realistic characteristics, it is limited in its ability to provide insight into the demographic dynamics of *Tribolium*. The next section describes a different modeling approach that sacrifices some biological realism in exchange for mathematical tractability.

3 Egg-Larval Submodel

In the Leslie matrix model of the preceding section, it was found that the cannibalism of eggs by larvae is destabilizing; this life-stage interaction drives the huge oscillations found in the immature age classes. By contrast to the dynamics of the immatures, the fluctuations in adult numbers are relatively small. A continuous-time model that focuses on the dynamics of the egg and larval life stages is called the "egg-larval submodel" (Hastings 1987; Hastings & Costantino 1987; Costantino & Desharnais 1991).

The egg-larval submodel is a special case of the McKendrick-von Foerster equation. This treatment of population growth, which was made popular by von Foerster (1959), is built on the work of Sharpe and Lotka (1911), Lotka (1925), and McKendrick (1926). If $n(x, t)$ denotes the number of individuals of age x at time t , the aging and death of the population is given by

$$\frac{\partial}{\partial t} n(x, t) + \frac{\partial}{\partial x} n(x, t) = -\mu(x, t) n(x, t), \quad (5)$$

where $\mu(x, t)$ is the mortality rate for an individual of age x at time t . Reproduction is expressed as a boundary condition, $n(0, t) = B(t)$, where $B(t)$ is the total birthrate of the population. Defining $b(x, t)$ as the number of offspring born to an individual of age x at time t , the total birthrate is computed using

$$B(t) = \int_0^{\omega} n(x, t) b(x, t) dx, \quad (6)$$

where ω is the maximum attainable age. To complete the model, one must also specify an initial age distribution $n(x, 0)$. In integral

form, the model can be written as

$$n(x, t) = \begin{cases} n(x-t, 0) \exp\left(-\int_{x-t}^x \mu(s, s+t-x) ds\right) & \text{for } t < x \leq \omega, \\ n(0, t-x) \exp\left(-\int_0^x \mu(s, s+t-x) ds\right) & \text{for } x \leq t. \end{cases} \quad (7)$$

The first expression is for the mortality of members of the initial population; the second is for individuals born after time $t = 0$. Webb (1985) provided detailed derivations and analyses of models of the McKendrick-von Foerster type.

The egg-larval submodel for flour beetles is based on two simplifying assumptions. First, it is assumed that the numbers of adults are constant and that these adults produce a steady supply of new eggs. The recruitment of new eggs into the population can be written as $n(0, t) = B$, where B is a constant representing the net rate at which new eggs are produced by adults. The second simplifying assumption is that the rate at which a larva eats eggs is independent of the age of the larva. This assumption is unrealistic because the cannibalistic voracity of larvae increases with size. Unfortunately, the analysis of the model becomes intractable with age-dependent rates of cannibalism. As a rough approximation, it will be assumed that all larvae eat eggs at a constant rate c . With these assumptions, the mortality rates of eggs and larvae are given by

$$\mu(x, t) = \begin{cases} \mu_E + cN_L(t) & \text{for } 0 < x \leq D_E, \\ \mu_L & \text{for } D_E < x \leq D_E + D_L, \end{cases} \quad (8)$$

where D_E and D_L are the durations of the egg and larval stages, respectively, μ_E and μ_L are the "natural" mortality rates for eggs and larvae, and the total number of larvae is given by

$$N_L(t) = \int_{D_E}^{D_E+D_L} n(x, t) dx. \quad (9)$$

Since pupae do not contribute to the mortality of eggs or larvae, they are excluded from the model. Assuming an initial population

of adults only, substitution of (8) into (7) gives

$$n(x, t) = \begin{cases} B \exp\left(-\mu_E - c \int_0^x N_L(t-s) ds\right) & \text{for } 0 \leq x < D_E, \\ n(D_E, t-x+D_E) \exp\left(-\mu_L(x-D_E)\right) & \text{for } D_E \leq x < D_E + D_L. \end{cases} \quad (10)$$

The first equation is for eggs, which must survive both natural mortality and cannibalism, and the second is for the natural mortality of larvae. Using (10) in (9) yields an integral equation for the total number of larvae:

$$N_L(t) = B \exp(-\mu_E D_E) \int_0^{D_L} \exp\left(-\mu_L y - c \int_0^{D_E} N_L(t-s-y) ds\right) dy, \quad (11)$$

where $y = x - D_E$ is the age of larvae from the time of hatching. This single integral equation can be used to investigate the dynamics of the model.

Hastings (1987) derived results for the equilibrium and local stability of (11) for the case where $\mu_L = 0$. He showed that a unique equilibrium exists whenever $B > 0$. This equilibrium is stable provided that

$$cB < \gamma \exp(\mu_E D_E + \gamma D_L D_E), \quad (12)$$

where γ is given by

$$\gamma = \theta^2 / [2 - \cos(D_E \theta) - \sin(D_L \theta)] \quad (13)$$

and $\theta = 2\pi / (D_E + D_L)$. Figure 3 is a plot of the stability boundaries for several egg-stage durations.

Hastings (1987) also derived results that describe the behavior of the model near the stability boundary. As the rate of cannibalism, c , or the birthrate, B , increases, the model undergoes a subcritical Hopf bifurcation at the point where the inequality (12) no longer holds. This means that in the neighborhood of the boundary, a stable equilibrium is surrounded by an unstable orbit. Initial conditions inside the unstable orbit approach the stable equilibrium; initial conditions outside the unstable orbit approach another attractor. The unstable orbit defines a local domain of attraction for the stable equilibrium. This implies the existence of multiple attractors for some subset of parameter space.

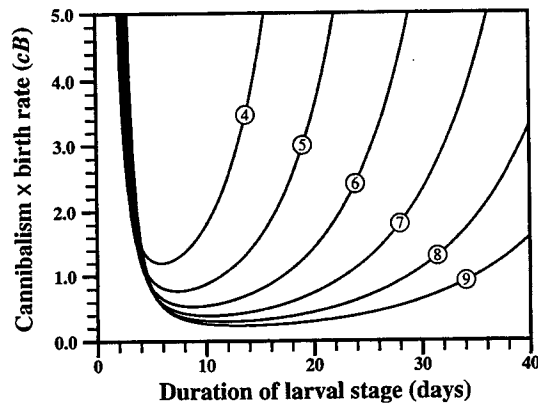


FIGURE 3. Stability boundaries of the egg-larval submodel from equation (12) with $\mu_E = 0$. Each curve is for a different duration of the egg stage (circled numbers). Parameter values below the curve result in a stable equilibrium.

Figure 4 shows two of the numerical results from a discretized analogue of the egg-larval submodel (Costantino & Desharnais 1991). The inner trajectory approaches a stable equilibrium point, and the outer trajectory approaches a stable limit cycle. Two stable attractors—a point equilibrium and a loop—coexist for the same parameter values. In fact, for the parameter values in this figure, multiple attractors are found for egg production rates in the range from $B = 134$ to $B = 424$. From a biological point of view, this is a significantly large region of parameter space.

The parameters of the egg-larval submodel can be estimated from experimental data. Park et al. (1961, 1964, 1965) published life-history and census data for four genetic strains of *T. confusum* (strains *bI-bIV*) and four genetic strains of *T. castaneum* (strains *cI-cIV*). From their results, estimates and standard errors were calculated for the parameters D_E , D_L , c , and B of the egg-larval submodel (for details, see Costantino & Desharnais 1991). Table 3 shows the dynamics predicted by the egg-larval submodel. Numerical simulations were used to determine the smallest value of the product cB at which a stable cycle persists; below this value, the equilibrium point is globally stable. Expressions (12) and (13) provide the bifurcation point for cB where the equilibrium loses stability. The interval bounded by these two values is a region of parameter space containing multiple attractors; a stable point and

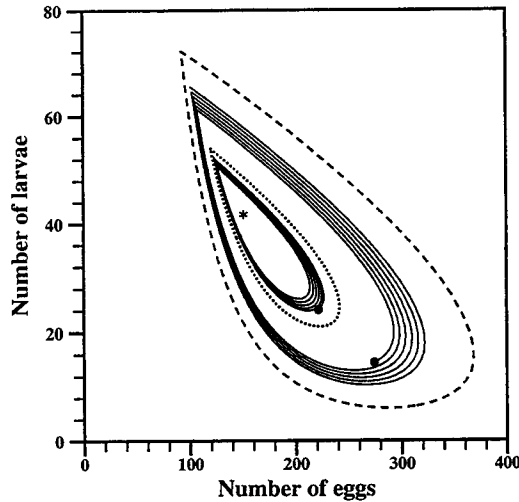


FIGURE 4. Simulations of the egg-larval submodel for $D_E = 4$ days, $D_L = 18$ days, $B = 150$ eggs/day, $c = 0.025$, and $\mu_E = \mu_L = 0$. The solid curves are trajectories with two different initial conditions (circles). The inner trajectory spirals toward the stable equilibrium (asterisk). The outer trajectory spirals toward a stable cycle (dashed loop). An unstable cycle (dotted loop) defines the domain of attraction of the stable equilibrium.

a stable orbit coexist. For values of cB above the bifurcation point, only a stable orbit is found. The estimated value of the product cB allows a classification of the predicted dynamics for the eight genetic strains. As this table indicates, all three possibilities are predicted: three of the strains have a globally stable point attractor, four of the strains are in the interval of multiple attractors, and a single strain, cI , is predicted to have only a stable orbit. This suggests that a rich spectrum of dynamic behaviors can be found in biologically relevant regions of parameter space.

The qualitative predictions of the egg-larval submodel are valid for less-restrictive assumptions. Although no larval mortality was assumed ($\mu_L = 0$), when this restriction is relaxed somewhat, a subcritical Hopf bifurcation is still predicted (Hastings 1987). A similar model with all four life stages has also been analyzed (Hastings & Costantino 1987; Costantino & Desharnais 1991). Expressions (12) and (13) give approximate stability bounds, and a region of multiple attractors still exists. Adding age-dependent egg canni-

TABLE 3. *Parameter Estimates and Dynamics Predicted by the Egg-Larval Submodel for Eight Genetic Strains of Tribolium*

Genetic Strain	D_E	D_L	Onset of Cycles (cB)	Bifurcation Point (cB)	Est'd Value (cB)	Predicted Dynamics
<i>bI</i>	5.37	18.96	1.60	2.60	0.75	stable point
<i>bII</i>	5.43	20.11	1.62	2.93	1.67	multiple attractors
<i>bIII</i>	5.63	18.89	1.41	2.06	1.01	stable point
<i>bIV</i>	5.60	19.92	1.48	2.45	1.54	multiple attractors
<i>cI</i>	4.09	17.58	3.13	8.51	30.32	stable orbit
<i>cII</i>	4.17	25.11	3.56	38.52	2.94	stable point
<i>cIII</i>	4.32	19.02	2.83	8.35	5.07	multiple attractors
<i>cIV</i>	4.19	20.93	3.28	14.96	3.75	multiple attractors

balism by larvae complicates the results (Costantino & Desharnais 1991). In general, a subcritical Hopf bifurcation does not always exist. However, if larval cannibalism rates increase quickly as larvae grow, then multiple attractors are found. Unfortunately, detailed information on age-specific cannibalism rates is needed to make predictions for any particular population.

4 Life-Stage Models

Recent efforts have concentrated on an interdisciplinary research program that integrates model derivation and analysis, parameter estimation and model verification, and design and implementation of biological experiments. The goal is to provide solid experimental evidence for a variety of nonlinear dynamic behaviors in flour beetle populations. Mathematical and statistical analyses are used to make a priori predictions concerning the range of dynamic behaviors; *Tribolium* experiments are designed to reveal transitions from one type of dynamic behavior to another. This section describes recent results and current efforts of the author and his collaborators (Costantino et al. 1995), which are based on this approach.

Discrete Generations

The simplest "life-stage" model of population growth is a discrete-generation model involving a single reproductive life stage. If $N(t)$ denotes the number of individuals in the reproductive life stage, then the population dynamics can be described using a simple difference equation of the form $N(t+1) = bN(t)f[N(t)]$, where b is the per capita reproductive rate and $f(N)$ is a "density-regulating factor" that depends on population size. A large number of functional forms for $f(N)$ have appeared in the literature (see, e.g., May & Oster 1976). For *Tribolium*, the function $f(N) = \zeta N^{\alpha-1} e^{-cN}$ attenuates population growth rates at high densities and allows for an "Allee effect" (Allee 1931) at low densities when $\alpha > 1$. The population growth model becomes

$$N(t+1) = \beta N(t)^\alpha \exp[-cN(t)], \quad (14)$$

where $\beta = b\zeta$. A graph of the right-hand side of (14) as a function of N shows a "one-humped curve" that is common to many population growth models. Typically, as the reproductive rate increases, these models undergo transitions from a stable equilibrium, to a period-doubling cascade (stable cycles of period 2, 4, 8, ...), to chaos, with bifurcations occurring at calculable critical points.

Parameter estimation and model evaluation make use of a stochastic analogue of the deterministic population model. At population sizes typical of flour beetle cultures, variability due to environmental fluctuations outweighs the component due to demographic fluctuations (Dennis & Costantino 1988). A characteristic of models with environmental variability is that noise is additive on a logarithmic scale (Dennis et al. 1991). Applying these ideas, the stochastic version of (14) is

$$N(t+1) = \beta N(t)^\alpha \exp[-cN(t) + Z(t)], \quad (15)$$

where $Z(t)$ has a normal distribution with a zero mean and variance σ^2 . It is assumed that there is no serial autocorrelation in the random components; that is, $Z(0), Z(1), Z(2), \dots$ are uncorrelated. This formulation preserves the deterministic model as the conditional expectation of $\ln N(t+1)$ given $N(t)$:

$$E[\ln N(t+1) \mid N(t) = n] = \ln[\beta n^\alpha \exp(-cn)]. \quad (16)$$

Each conditional "one-step" transition can be treated as an independent observation for the purposes of parameter estimation and model evaluation.

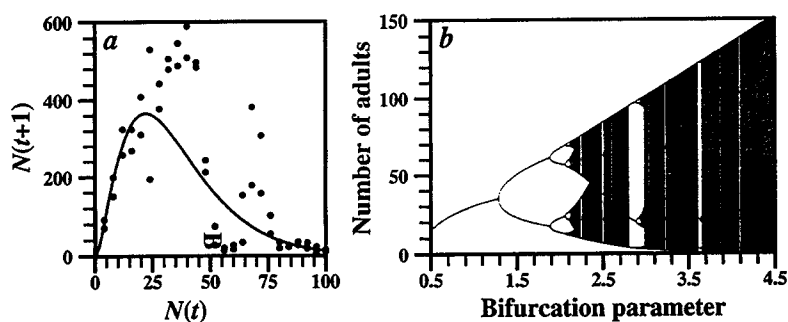


FIGURE 5. Results of the pilot study of the discrete-generation model (14). (a) The numbers of adults recovered plotted against the numbers of adults from the preceding generation; the smooth curve is based on equation (14) with the maximum-likelihood parameter estimates. (b) Predicted bifurcation diagram for the populations with β as the bifurcation parameter.

Flour beetles can be cultured to mimic the discrete-generation life history implied by (14). Adults are placed in fresh medium and allowed to oviposit for a fixed interval of time called the "breeding interval." At the end of the breeding interval, all adults are removed and the medium containing eggs is returned to the vials. Five weeks later, the flour is sifted and the next generation of adults is counted. The immatures that do not reach adulthood are discarded. The new adults are placed in fresh medium to initiate another generation. By altering the duration of the breeding interval, one can control the rate of reproduction.

A pilot study was conducted to investigate the potential of this experimental protocol for studying discrete-generation population dynamics. A fixed number of adults of the *sooty* strain of *T. castaneum* was placed into vials containing 20 grams of medium. Adult numbers ranged from 4, 8, 12, . . . , to 100 for a total of 25 treatments. Each adult density was repeated. After a breeding interval of seven days, the adults were removed and the offspring were allowed to develop for five weeks.

The results of the pilot study are plotted in Figure 5. The data are the equivalent of a one-dimensional map of adult numbers in two consecutive generations (Fig. 5a). The model (15) was fitted to the data using the method of maximum likelihood. Parameter estimates of $\beta = 10.8$, $\alpha = 1.68$, and $c = 0.076$ were obtained. Figure 5b shows the predicted dynamics as a bifurcation diagram with β as the bifurcation parameter. The ordinate represents the

asymptotic values of adult number for a given value of β , with the remaining parameters fixed at their estimated values. For small values of β , a stable equilibrium is predicted. As β increases, this equilibrium bifurcates into a stable 2-cycle. The 2-cycle gives way to a 4-cycle, 8-cycle, etc., until acyclic chaotic dynamics appear. Within the chaotic region are intervals of "period locking." Note that the estimated value of $\beta = 10.8$ places the experimental populations well within the chaotic region.

This protocol opens the opportunity of documenting experimentally transitions in dynamic behavior. By shortening the breeding interval, one can decrease the value of β . With an array of experimental treatments, it should be possible to cover the sequence of dynamic behavior from stable equilibria, to period doublings, to chaos. Such experiments are currently under way.

Overlapping Generations

A structured model is required to account for population dynamics in the case of overlapping generations. These are coupled difference equations or matrix equations that describe the dynamics of two or more life stages or groupings of life stages (Cushing 1988; Caswell 1989). Dennis et al. (1995) have proposed the use of three coupled difference equations to describe the dynamics of larvae, pupae, and adults in *Tribolium* cultures:

$$L(t+1) = bA(t) \exp \left[-c_{EA}A(t) - c_{EL}L(t) \right], \quad (17a)$$

$$P(t+1) = L(t)(1 - \mu_L), \quad (17b)$$

$$A(t+1) = P(t) \exp \left[-c_{PA}A(t) \right] + A(t)(1 - \mu_A). \quad (17c)$$

Here $L(t)$ refers to the number of feeding larvae, $P(t)$ refers to the number of nonfeeding larvae, pupae, and callow adults, and $A(t)$ refers to the number of reproductive adults. The unit of time is taken to be the maturation interval for feeding larvae, so that after one unit of time either a larva dies or it survives and pupates. This unit of time is also the cumulative time spent as a nonfeeding larva (sometimes called a "prepupa"), pupa, and callow adult. The quantity b (> 0) is the number of larval recruits per adult per unit of time in the absence of cannibalism. The fractions μ_L and μ_A are the larval and adult probabilities, respectively, of dying from causes other than cannibalism. The exponential nonlinearities account for the cannibalism of eggs by both adults and larvae and

the cannibalism of pupae by adults (Fig. 1). It is assumed that the only significant source of pupal mortality is cannibalism by adults. Dennis et al. (1995) referred to this model as the "LPA model."

Adding noise on a logarithmic scale produces the following stochastic model:

$$L(t+1) = bA(t) \exp[-c_{EA}A(t) - c_{EL}L(t) + Z_1(t)], \quad (18a)$$

$$P(t+1) = L(t)(1 - \mu_L) \exp[Z_2(t)], \quad (18b)$$

$$A(t+1) = \left\{ P(t) \exp[-c_{PA}A(t)] + A(t)(1 - \mu_A) \right\} \times \exp[Z_3(t)]. \quad (18c)$$

The random vector $\mathbf{Z}(t) = (Z_1(t), Z_2(t), Z_3(t))$ is assumed to have a trivariate normal distribution with mean vector of $\mathbf{0}$ and a covariance matrix of Σ . Including covariance terms in the off-diagonal elements of Σ allows for the possibility of correlations in the growth fluctuations among the life stages during the same time intervals. However, we assume the correlations between time intervals to be small by comparison; that is, $\mathbf{Z}(0), \mathbf{Z}(1), \mathbf{Z}(2), \dots$ are uncorrelated.

The dynamics of the deterministic model (17) are preserved by the stochastic model (18) as conditional expectations on a logarithmic scale:

$$E[\ln L(t+1)] = \ln[ba \exp(-c_{EA}a - c_{EL}\ell)], \quad (19a)$$

$$E[\ln P(t+1)] = \ln[\ell(1 - \mu_L)], \quad (19b)$$

$$E[\ln A(t+1)] = \ln[p \exp(-c_{PA}a) + a(1 - \mu_A)], \quad (19c)$$

given that $L(t) = \ell$, $P(t) = p$, and $A(t) = a$. This result allows an explicit connection between the mathematical model and the population time-series data. Given the numbers of each life stage at time t and estimates for the model parameters, one can predict the expected numbers of each life stage at time $t+1$ (two weeks later). Using the stochastic model (18), one can choose a set of parameter values that maximizes the joint probability of the one-time-step transitions in the observed time series. The model is connected to the data by one-step forecasts, not by continued iteration.

Dennis et al. (1995) have applied this maximum-likelihood procedure to earlier data on the *cos* genetic strain of *T. castaneum* (De-sharnais & Costantino 1980). They used the 4 control cultures for parameter estimation and the 9 cultures subjected to demographic perturbations for model evaluation. Sophisticated diagnostics were conducted on the residuals. The LPA model (17) did a remarkably good job of predicting the dynamics of all 13 populations. Partic-

TABLE 4. *Parameter Estimates for the LPA Model*

Parameter	Estimate	95% Confidence Interval
b	11.7	(6.2, 22.2)
μ_A	0.11	(0.07, 0.15)
μ_L	0.51	(0.43, 0.58)
c_{EA}	0.011	(0.004, 0.180)
c_{EL}	0.009	(0.008, 0.011)
c_{PA}	0.018	(0.015, 0.021)

ularly impressive was the fact that a single set of parameter values from the control cultures was able to describe the dynamics of the 9 demographically manipulated cultures, even though none of the data from these manipulated populations was used to obtain the parameter estimates.

Maximum-likelihood parameter estimates for the LPA model are given in Table 4. The 95 percent confidence intervals are based on profile likelihoods (McCullagh & Nelder 1989). When these parameter values are substituted into (17), the model simulations approach a stable 2-cycle.

Figure 6 shows the one-step predictions (Desharnais & Costantino 1980, control replicate "A"). Keep in mind that a single set of parameter values is used for all the predictions. The model does a particularly good job of prediction in the region of strong oscillations. Dennis et al. (1995) provided similar plots for all 13 populations.

Equilibrium densities and stability boundaries can be obtained numerically for the LPA model. Although no closed-form solution exists for the equilibrium densities of each life stage, it can be shown that a single unique nontrivial equilibrium exists provided that $b > \mu_A / (1 - \mu_L)$ (Dennis et al. 1995). This equilibrium can be found numerically by locating the unique real root of a simple nonlinear equation. The 3×3 linearized stability matrix \mathbf{S} can be expressed in terms of the model's parameters and equilibrium densities. Given parameter values and the corresponding equilibrium life-stage densities, the eigenvalues of \mathbf{S} can be computed. If the moduli of these three eigenvalues are all less than unity, the equilibrium is stable. This process can be repeated for different combinations of parameter values to map out the stability boundaries in parameter space.

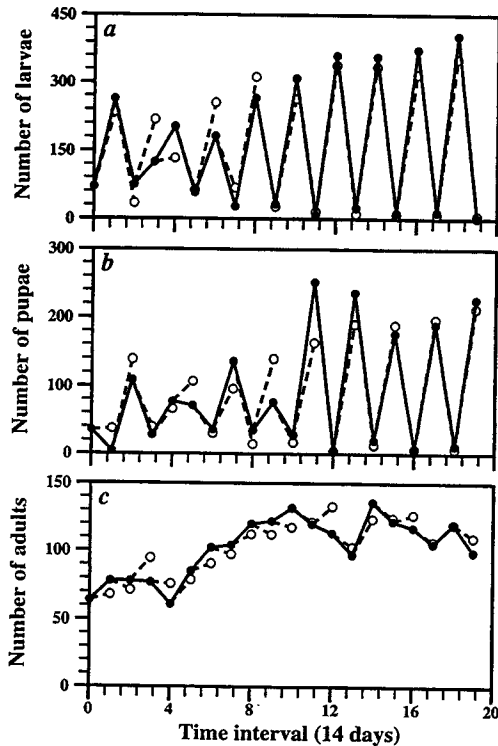


FIGURE 6. Densities of (a) larvae, (b) pupae, and (c) adults (*Desharnais & Costantino 1980*, control replicate "A"). Solid circles, Census points; open circles, one-step forecasts.

Figure 7 shows the stability boundaries of the LPA model as functions of the adult mortality rate, μ_A , and the rate of egg cannibalism by larvae, c_{EL} . For this figure, the remaining parameters of the LPA model were set at their estimated values (Table 4). Crossing the stability boundary to the left of the large peak represents a bifurcation into a stable 2-cycle. Here, a single real dominant eigenvalue of \mathbf{S} becomes equal to -1 . Asymptotically, life-stage densities oscillate between two discrete values. Crossing the stability boundary to the right of this peak represents a bifurcation into an invariant loop. Here \mathbf{S} has a pair of complex conjugate eigenvalues of modulus one. Asymptotically, life-stage densities move aperiodically around a closed loop. The solid circle in Figure 7 shows the location of the *cos* genetic strain of *T. castaneum* in

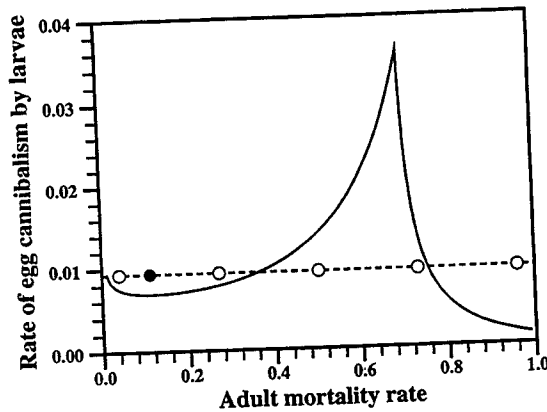


FIGURE 7. Stability boundaries for the LPA model (17) as a function of the adult mortality rate and the rate of egg cannibalism by larvae. The remaining parameters were set at the estimated values for the *cos* strain of *T. castaneum*. Solid circle, Location of the *cos* strain in parameter space; open circles, adult mortality treatments in an experimental study now under way.

the unstable region of parameter space near the 2-cycle boundary. Its location in parameter space is consistent with the demographic dynamics observed in Figure 6.

The stability boundary in Figure 7 has stimulated new experiments. In a recent study (Costantino et al. 1995), adult mortality rates were manipulated by removing or adding adults at the time of census to make the total number of adults that died during an interval consistent with a predetermined value of μ_A . In addition to a control (no manipulation), values of μ_A were chosen to be 0.04, 0.27, 0.50, 0.73, and 0.96 (Fig. 7, open circles). This experimental design was implemented using two different genetic strains of *T. castaneum*. There were four replicates for each combination of adult mortality rate and genetic strain.

The predicted outcomes from this experimental design are visualized in Figure 8. This bifurcation diagram was obtained by iterating the deterministic LPA model for different values of μ_A , with the remaining parameters fixed at their estimated values (Table 4). This graph shows the asymptotic behavior of the LPA model as one moves along the dashed line in Figure 7. At very low adult

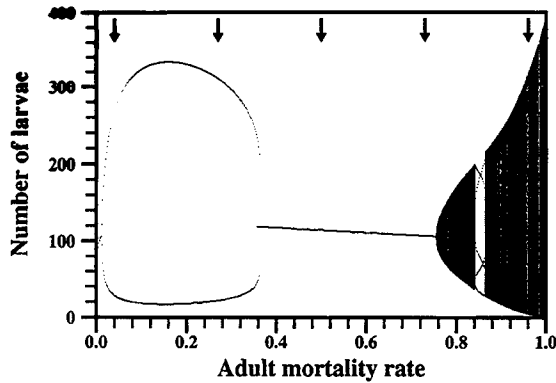


FIGURE 8. A bifurcation diagram for the LPA model (17) with adult mortality rate as the bifurcation parameter. The remaining parameters were set at the estimated values for the *cos* strain of *T. castaneum*. Arrows show the adult mortality treatments of Costantino et al. (1995).

mortalities, there is a stable point equilibrium, but this equilibrium soon bifurcates into a stable 2-cycle. This 2-cycle is followed by a narrow region of multiple attractors ($0.357 \leq \mu_A \leq 0.363$) where stable equilibria coexist with stable 2-cycles. As μ_A increases, positive equilibria persist, whereas the stable 2-cycles disappear. At high values of adult mortality, there is a bifurcation to an invariant loop. Adult-mortality treatments were chosen to sample these different dynamic behaviors (Fig. 7, *open circles*; Fig. 8, *arrows*). The goal is to provide convincing evidence for nonlinear population dynamics by documenting transitions in the demographic behavior of experimental populations. For the results of this study, see Costantino et al. (1995).

5 Concluding Remarks

The research results described in this chapter are joined by a common theme: the integration of theoretical and experimental approaches in order to study nonlinear dynamics in structured populations. In this regard, the *Tribolium* experimental system provides many opportunities. This animal model shows the potential for exhibiting many of the exotic behaviors so far identified only in theoretical models: discrete-point cycles, limit cycles, invariant loops, multiple attractors, strange attractors, chaos. Through a

careful choice of species, genetic strains, environmental conditions, and husbandry protocols, one can "sample" parameter space experimentally, obtaining populations that cover the entire spectrum of dynamic behaviors. The possibility exists for "nudging" populations across boundaries within parameter space, documenting experimentally transitions in behavior. If multiple attractors are predicted, a variety of initial conditions could be used to seek out the attractors. If multiple attractors are found, perturbations could be used to shift a population from one domain of attraction to another. This work is only beginning. The prospects are exciting.

Acknowledgments

The research described in this chapter was supported in part by U.S. National Science Foundation grants DMS-9206678, DMS-9306271, and DMS-9319073.

Literature Cited

- Allee, W. C. 1931. *Animal Aggregations*. University of Chicago Press.
- Bell, A. E. 1982. The *Tribolium* model and animal breeding. *Second World Congress on Genetics and Applications to Livestock Production* 5: 26-42.
- Bernardelli, H. 1941. Population waves. *Journal of the Burma Research Society* 31: 1-18.
- Caswell, H. 1989. *Matrix Population Models*. Sinauer, Sunderland, Mass.
- Chapman, R. N. 1928. Quantitative analysis of environmental factors. *Ecology* 9: 111-122.
- Costantino, R. F., and R. A. Desharnais. 1991. *Population Dynamics and the 'Tribolium' Model: Genetics and Demography*. Springer-Verlag, New York.
- Costantino, R. F., J. M. Cushing, B. Dennis, and R. A. Desharnais. 1995. Experimentally induced transitions in the dynamic behaviour of insect populations. *Nature* 375: 227-230.
- Cushing, J. M. 1988. Nonlinear matrix models and population dynamics. *Natural Resource Modelling* 2: 539-580.
- Cushing, J. M., B. Dennis, R. A. Desharnais, and R. F. Costantino. In press. An interdisciplinary approach to understanding nonlinear ecological dynamics. *Ecological Modelling*.
- Dennis, B., and R. F. Costantino. 1988. Analysis of steady-state populations with the gamma abundance model and its application to *Tribolium*. *Ecology* 69: 1200-1213.
- Dennis, B., P. L. Munholland, and J. M. Scott. 1991. Estimation of growth and extinction parameters for endangered species. *Ecological Monographs* 61: 115-143.

- Dennis, B., R. A. Desharnais, J. M. Cushing, and R. F. Costantino. 1995. **Nonlinear demographic dynamics: Mathematical models, statistical methods and biological experiments.** *Ecological Monographs* 65: 261-281.
- Desharnais, R. A., and R. F. Costantino. 1980. Genetic analysis of a population of *Tribolium*. VII. Stability: Response to genetic and demographic perturbations. *Canadian Journal of Genetics and Cytology* 22: 577-589.
- Desharnais, R. A., and L. Liu. 1987. Stable demographic limit cycles in laboratory populations of *Tribolium castaneum*. *Journal of Animal Ecology* 56: 885-906.
- Hastings, A. 1987. Cycles in cannibalistic egg-larval interactions. *Journal of Mathematical Biology* 24: 651-666.
- Hastings, A., and R. F. Costantino. 1987. Cannibalistic egg-larva interactions in *Tribolium*: An explanation for the oscillations in population numbers. *American Naturalist* 130: 36-52.
- Jillson, D., and R. F. Costantino. 1980. Growth, distribution, and competition of *Tribolium castaneum* and *Tribolium brevicornis* in fine-grained habitats. *American Naturalist* 116: 206-219.
- King, C. E., and P. S. Dawson. 1972. Population biology and the *Tribolium* model. *Evolutionary Biology* 5: 133-227.
- Leslie, P. H. 1945. On the use of matrices in certain population mathematics. *Biometrika* 33: 183-212.
- Lewis, E. G. 1942. On the generation and growth of a population. *Sankhya* 6: 93-96.
- Lotka, A. J. 1925. *Elements of Physical Biology*. Williams & Wilkins, Baltimore.
- May, R. M., and G. F. Oster. 1976. Bifurcations and dynamic complexity in simple ecological models. *American Naturalist* 110: 573-599.
- McCullagh, P., and J. A. Nelder. 1989. *Generalized Linear Models*. Chapman & Hall, London.
- McKendrick, A. G. 1926. Applications of mathematics to medical problems. *Proceedings of the Edinboro Mathematical Society* 54: 98-130.
- Mertz, D. B. 1972. The *Tribolium* model and the mathematics of population growth. *Annual Review of Ecology and Systematics* 3: 51-78.
- Moffa, A. M. 1976. Genetic Polymorphism and Demographic Equilibrium in *Tribolium castaneum*. Ph.D. diss. University of Rhode Island, Kingston.
- Park, T. 1948. Experimental studies of interspecies competition. I. Competition between populations of the flour beetles *Tribolium confusum* Duval and *Tribolium castaneum* Herbst. *Ecological Monographs* 18: 265-308.
- Park, T., D. B. Mertz, and K. Petruszewicz. 1961. Genetic strains of *Tribolium*: Their primary characteristics. *Physiological Zoology* 34: 62-80.
- Park, T., P. H. Leslie, and D. B. Mertz. 1964. Genetic strains and competition in populations of *Tribolium*. *Physiological Zoology* 37: 97-162.

- Park, T., D. B. Mertz, W. Grodzinski, and T. Prus. 1965. Cannibalistic predation in populations of flour beetles. *Physiological Zoology* 38: 289-321.
- Rich, E. L. 1956. Egg cannibalism and fecundity in *Tribolium*. *Ecology* 37: 109-120.
- Sharpe, F. R., and A. J. Lotka. 1911. A problem in age-distribution. *Philosophy Magazine* 21: 435-438.
- Sokoloff, A. 1972. *The Biology of 'Tribolium.'* Vol. 1. Oxford University Press.
- . 1974. *The Biology of 'Tribolium.'* Vol. 2. Oxford University Press.
- . 1977. *The Biology of 'Tribolium.'* Vol. 3. Oxford University Press.
- Stanley, J. 1932. A mathematical theory of the growth of populations of the flour beetle, *Tribolium confusum* Duval. *Canadian Journal of Research* 6: 632-671.
- von Foerster, H. 1959. Some remarks on changing populations. Pp. 382-407 in F. Stohlman, ed., *The Kinetics of Cellular Proliferation*. Grune & Stratton, New York.
- Webb, G. F. 1985. *Theory of Nonlinear Age-Dependent Population Dynamics*. Marcel Dekker, New York.